Supplementary Material

A computational chemical study of the chemical reactivity of naratriptan through global and local descriptors derived from DFT.

WENDOLYNE LÓPEZ-OROZCO[1], CLARA HILDA RIOS REYES[2], LUIS HUMBERTO MENDOZA HUIZAR[1,]*.

[1]*Universidad Autónoma del Estado de Hidalgo. Academic Area of Chemistry. Carretera Pachuca-Tulancingo Km. 4.5 Mineral de la Reforma, Hgo, México.*

[2]*Universidad Lasalle Pachuca, Calle Belisario Domínguez 202, Centro, 42000 Pachuca de Soto, Hgo. México.*

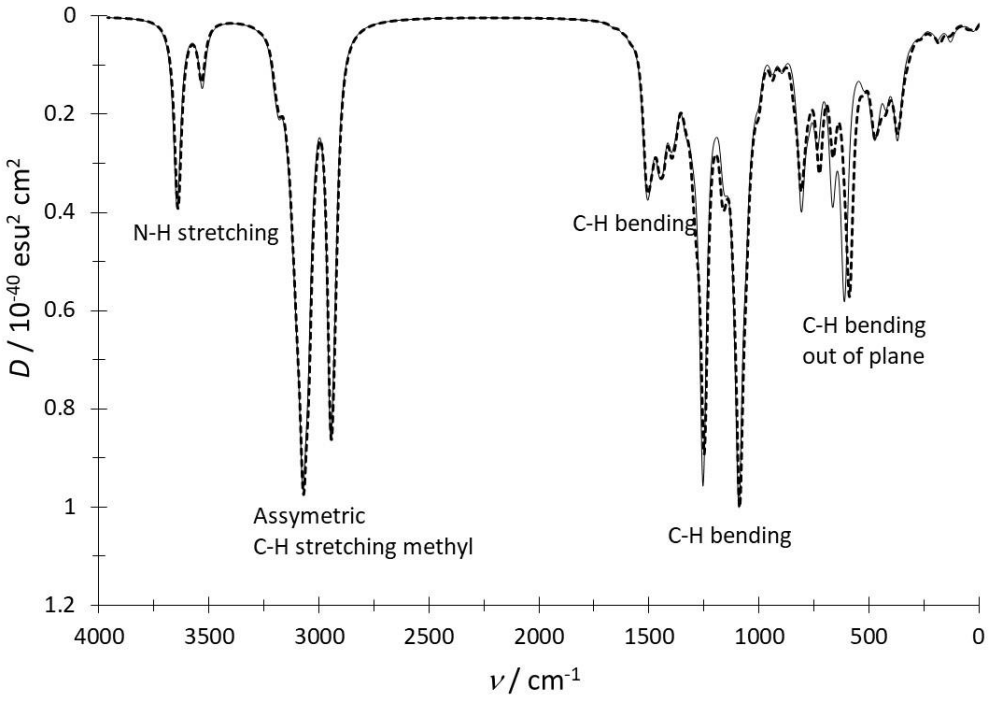

Figure 1S. Theoretical IR spectra of Nar–I (solid line) and Nar-II (broken line) in the aqueous phase obtained at the B3LYP/DGDZVP level of theory.

*Corresponding author. E-mail: hhuizar@uaeh.edu.mx

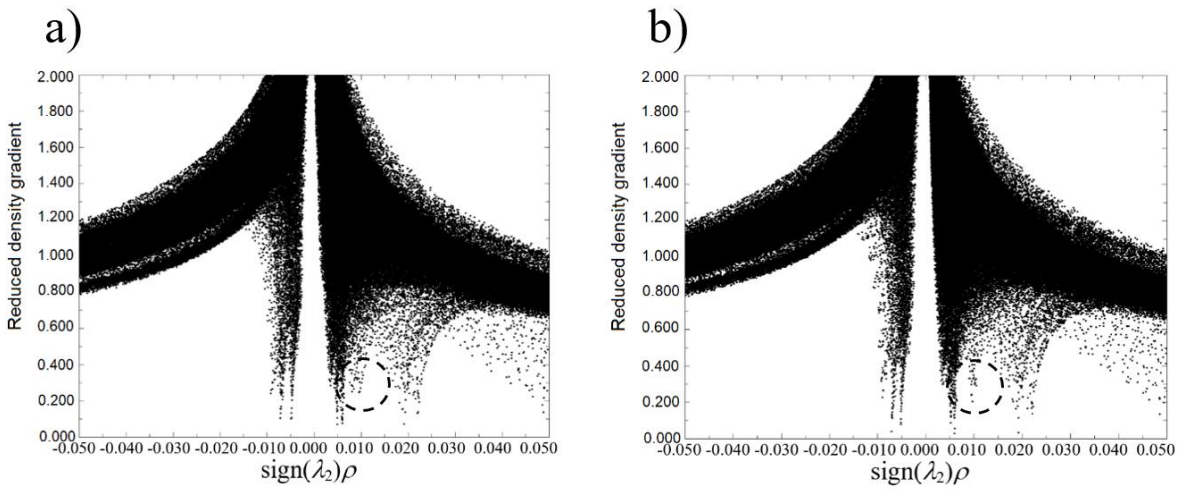

Figure 2S. Plots of the reduced density gradient vs sign(λ_2)ρ for a) Nar-I and b) Nar-II. Broken circles indicate the main differences between both plots.

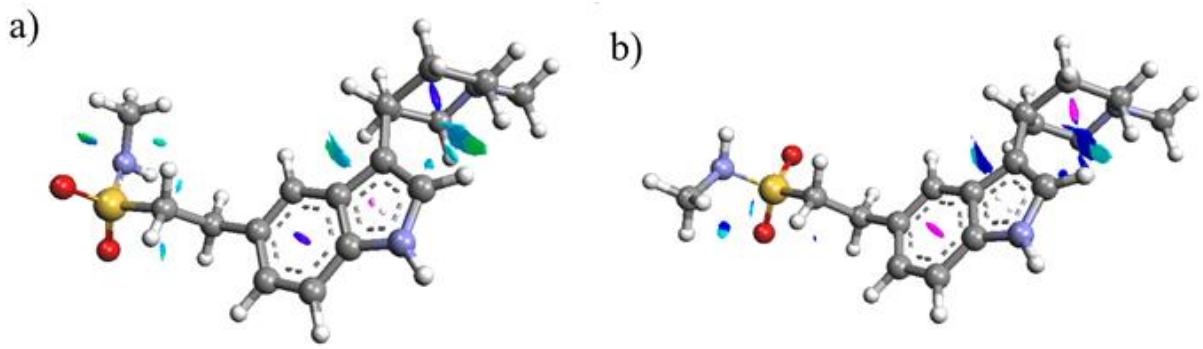

Figure 3S. NCI Isosurfaces ρ = 0.2 for a) Nar-I and (b) Nar-II in the aqueous phase.

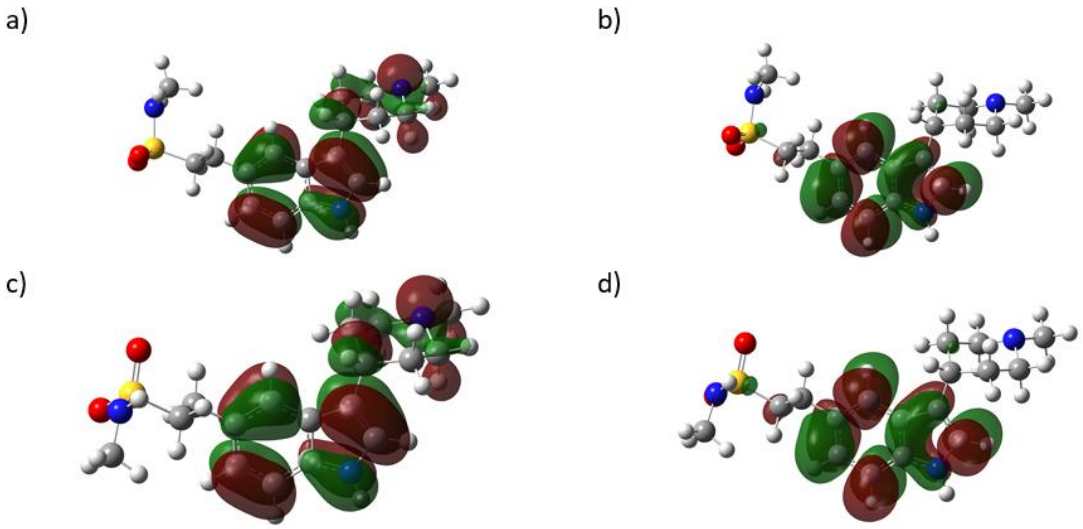

Figure 4S*. HOMO and LUMO's distributions on Nar-I and Nar-II obtained at the B3LYP/DGDZVP level of theory in the aqueous phase employing the PCM solvation model. In all cases the isosurfaces were obtained at 0.08 e/u.a.*[3]

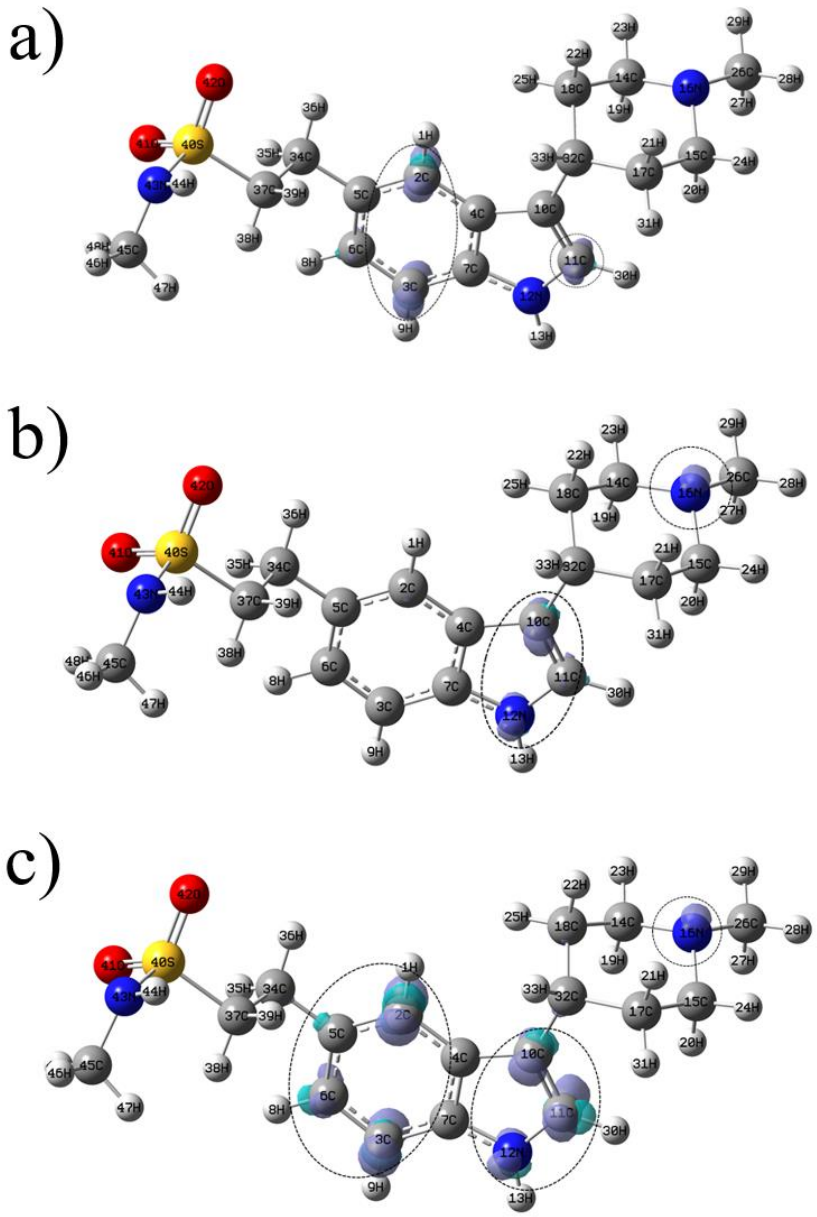

Figure 5S. Isosurfaces of the Fukui Functions for Nar-II according to equations (10), (11) and (12) at the B3LYP/DGDZVP level of theory employing the PCM solvation model. In the case of (a) nucleophilic, b) electrophilic and c) free radical attacks. In all cases the isosurfaces were obtained at 0.008 e/u.a.^{3}, broken circles show the more reactive zones in each molecule.

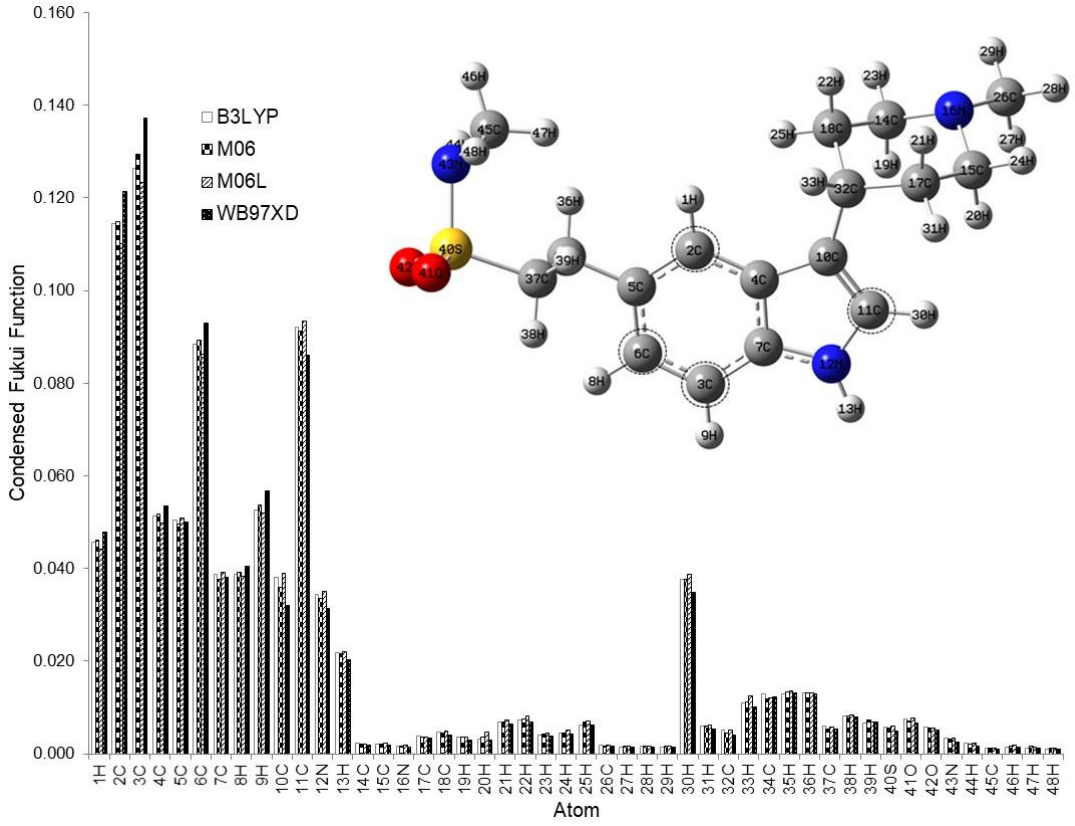

Figure 6S. Condensed Fukui Function values for nucleophilic attacks on Nar-I at the X/ DGDZVP (where X=B3LYP, M06, M06L and WB97XD) level of theory, in the aqueous phase employing Hirshfeld population and equations (13)-(15), broken circles show the more reactive zones in each molecule.

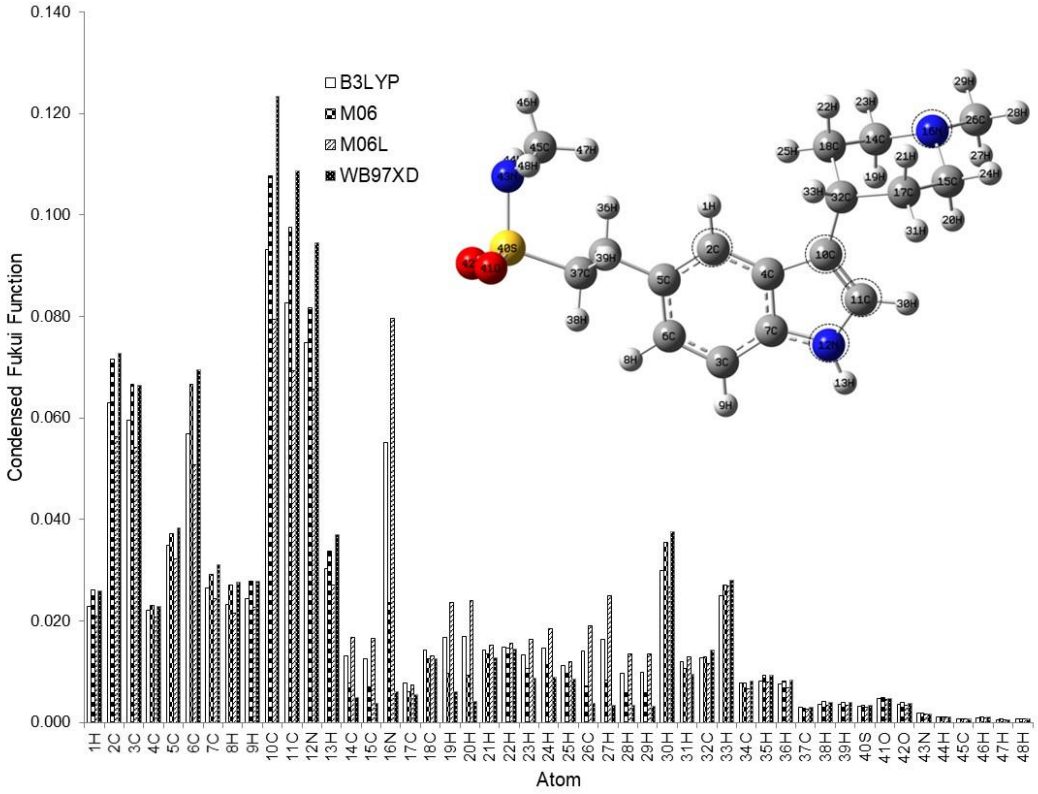

48

49 **Figure 7S.** Condensed Fukui Function values for electrophilic attacks on Nar-I at the X/DGDZVP
50 (where X=B3LYP, M06, M06L and WB97XD) level of theory, in the aqueous phase employing
51 Hirshfeld population and equations (13)-(15), broken circles show the more reactive zones in each
52 molecule.

53

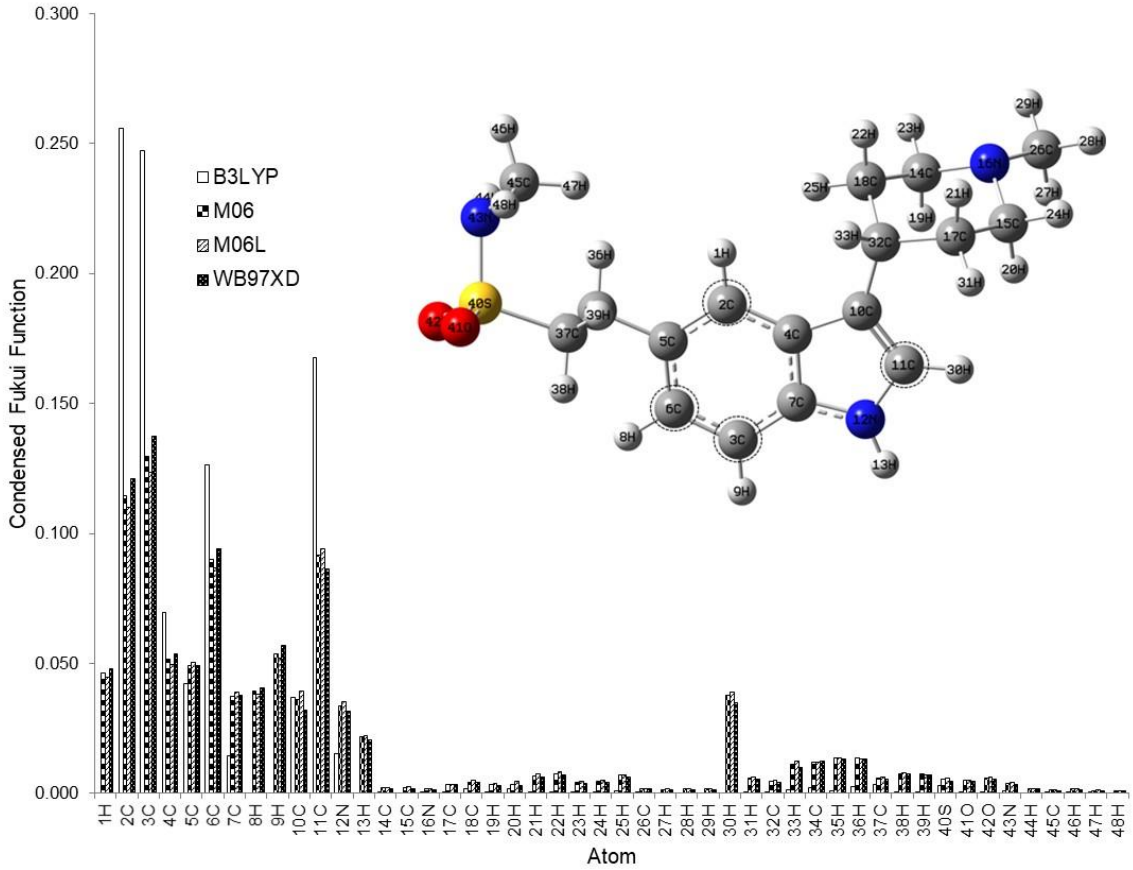

54

55 **Figure 8S.** Condensed Fukui Function values for free radical attacks on Nar-I at the X/DGDZVP
56 (where X=B3LYP, M06, M06L and WB97XD) level of theory, in the aqueous phase employing
57 Hirshfeld population and equations (13)-(15), broken circles show the more reactive zones in each
58 molecule.

59

60

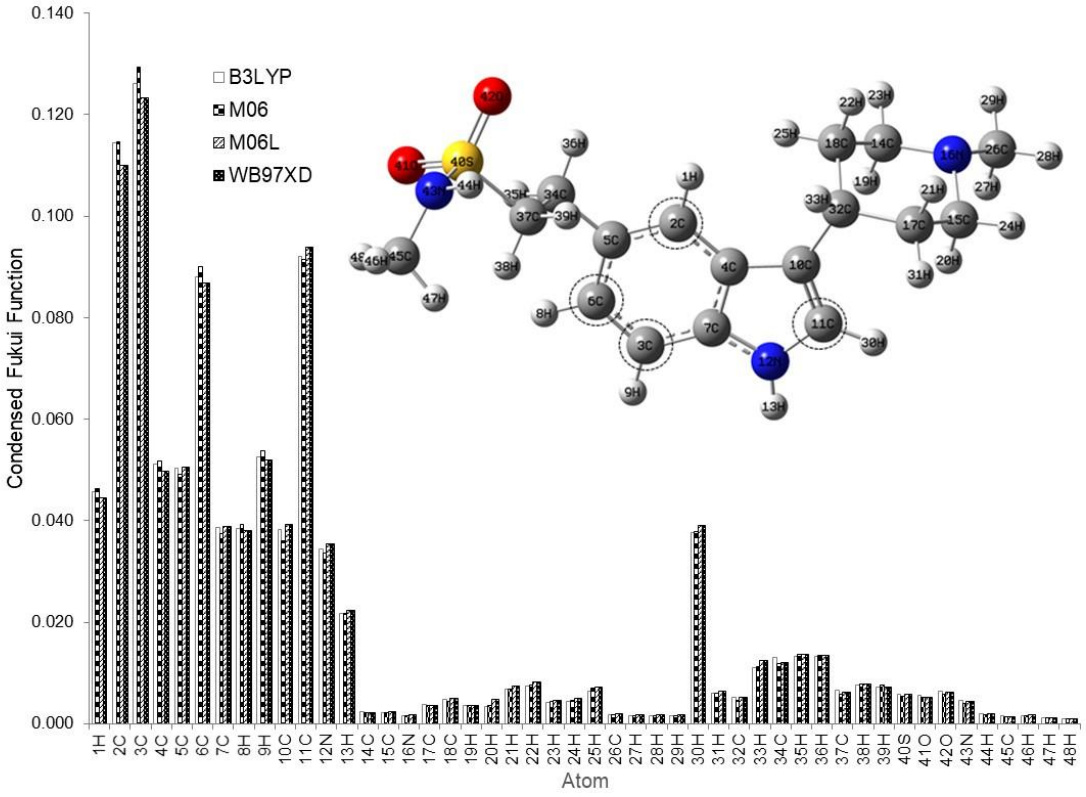

Figure 9S. Condensed Fukui Function values for nucleophilic attacks on Nar-II at the X/DGDZVP (where X=B3LYP, M06, M06L and WB97XD) level of theory, in the aqueous phase employing Hirshfeld population and equations (13)-(15), broken circles show the more reactive zones in each molecule.

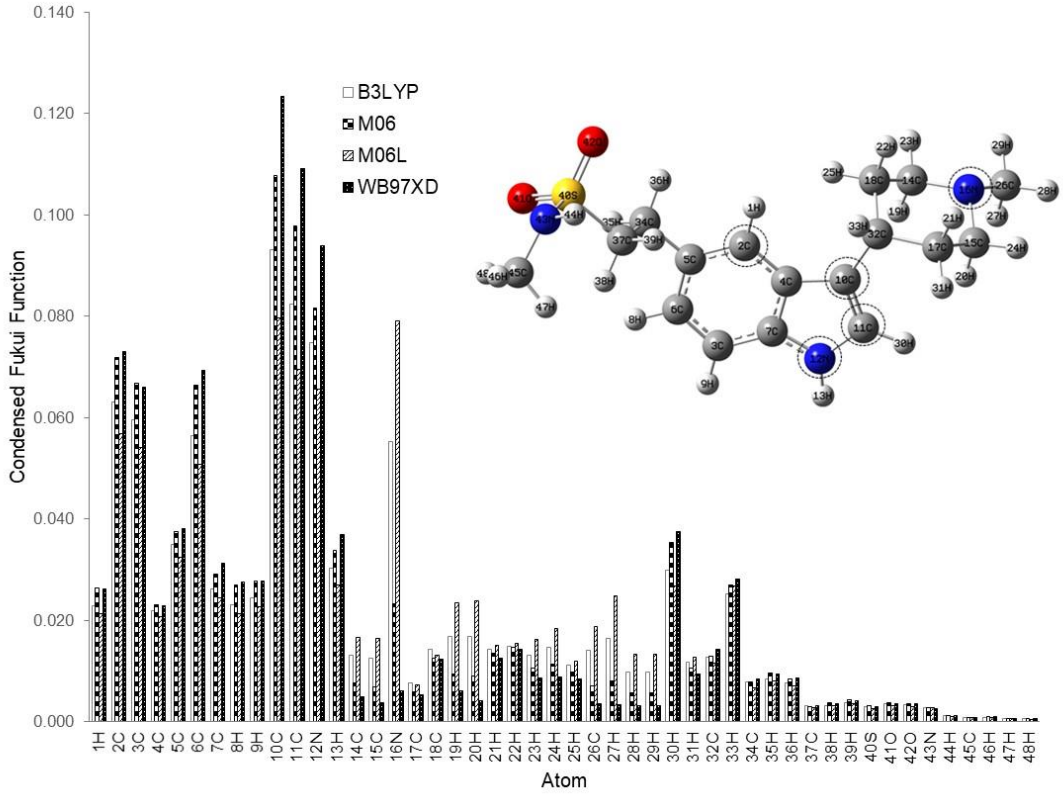

Figure 10S. Condensed Fukui Function values for electrophilic attacks on Nar-II at the X/DGDZVP (where X=B3LYP, M06, M06L and WB97XD) level of theory, in the aqueous phase employing Hirshfeld population and equations (13)-(15), broken circles show the more reactive zones in each molecule.

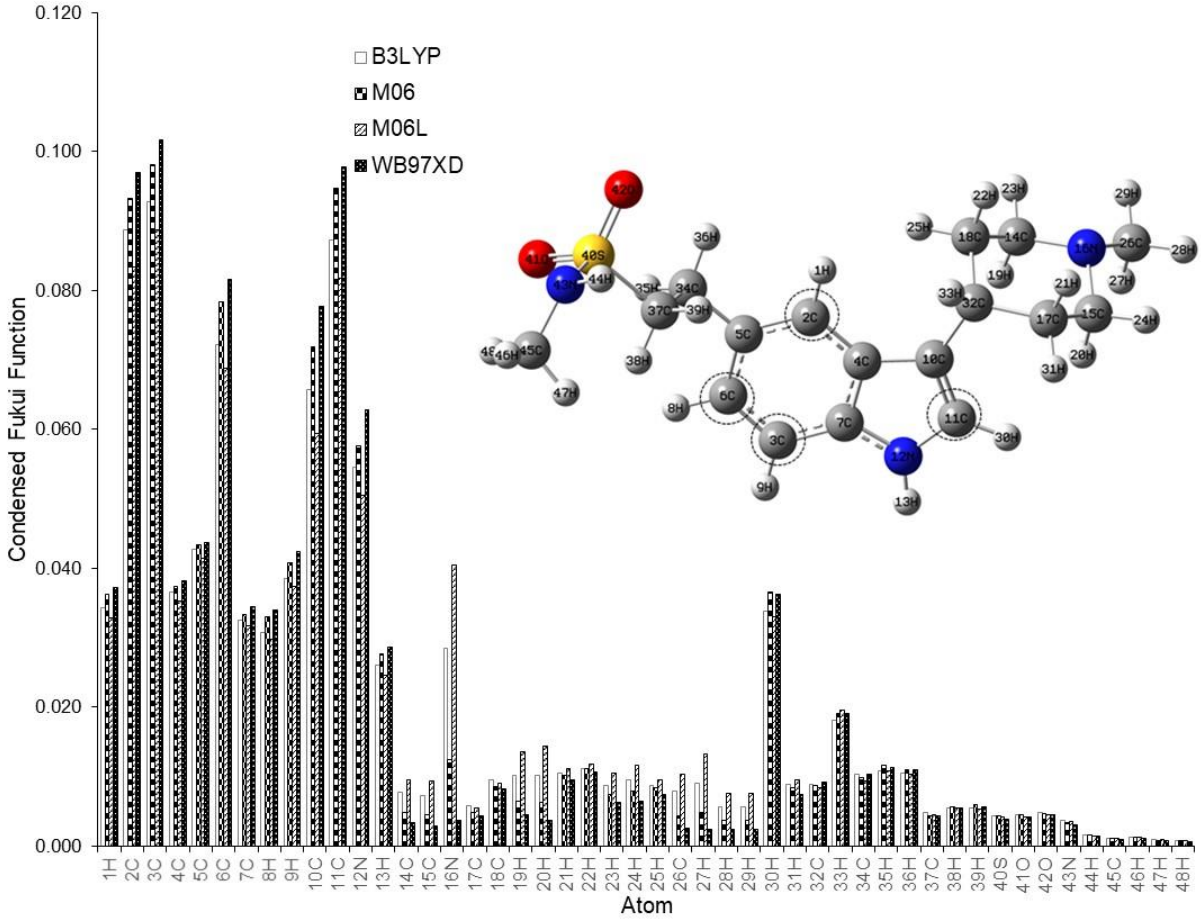

Figure 11S. Condensed Fukui Function values for free radical attacks on Nar-II at the X/DGDZVP (where X=B3LYP, M06, M06L and WB97XD) level of theory, in the aqueous phase employing Hirshfeld population and equations (13)-(15), broken circles show the more reactive zones in each molecule.

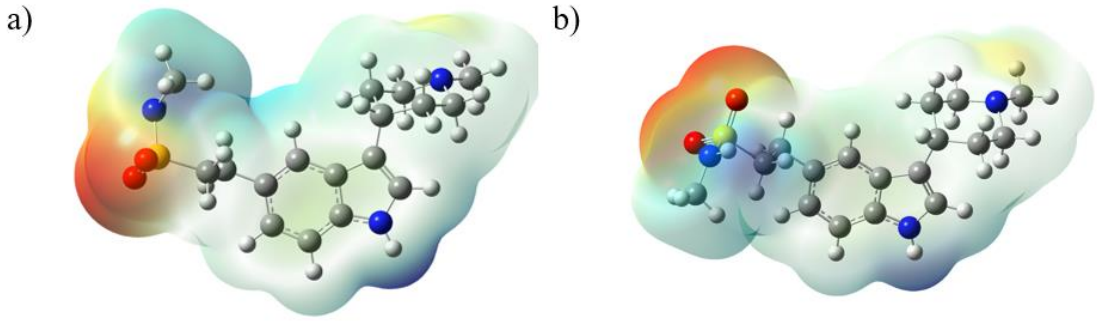

Figure 12S. Mapping of the electrostatic potentials evaluated at the b3lyp/DGDZVP level of theory employing the PCM solvation model, onto a density isosurface (value =0.002 e/a.u.^{3}) for a) Nar-I, b) Nar-II.

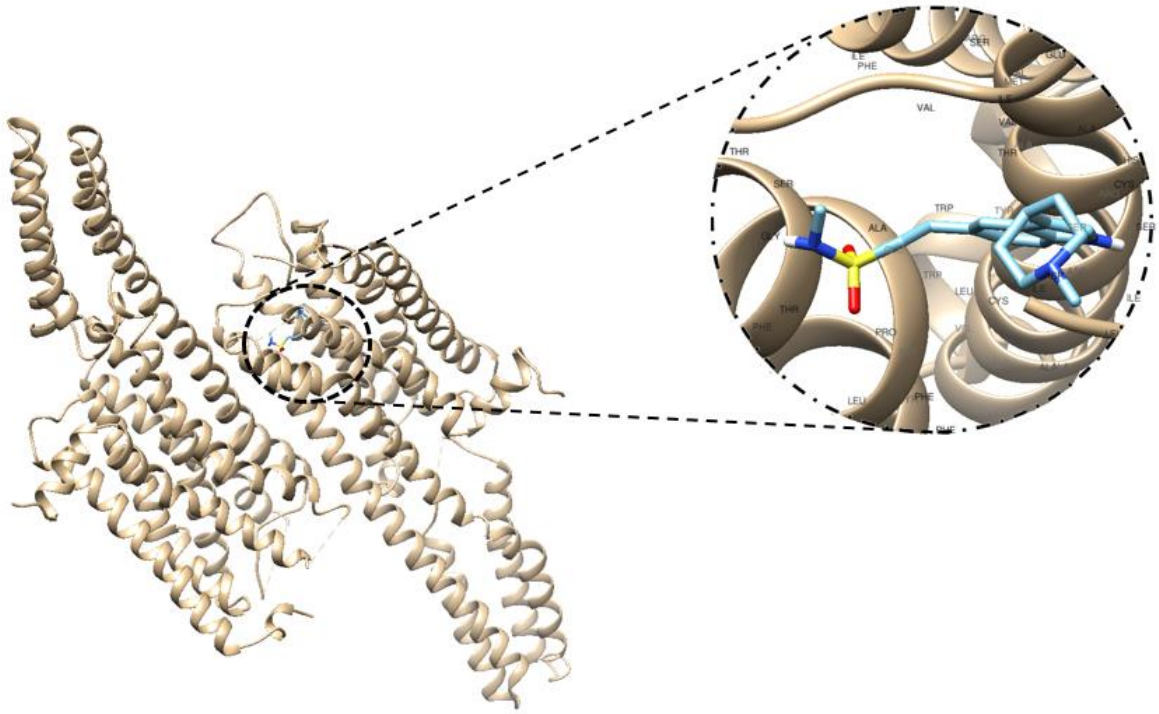

Figure 13S. Binding site of Nar-I on the $5HT_{1B}$ receptor.

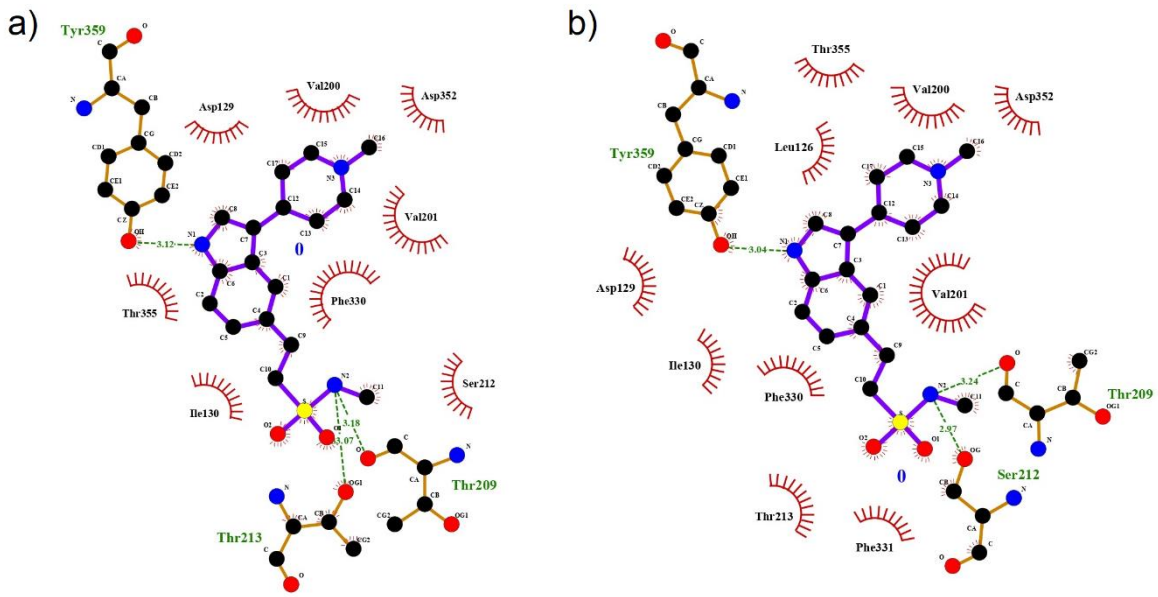

Figure 14S. 2D ligand interaction diagram for a) Nar-I/5HT$_{1B}$ and b) Nar-II/5HT$_{1B}$.